Bo-Hua Sun[1]

[1]School of Civil Engineering & Institute of Mechanics and Technology
Xian University of Architecture and Technology, Xian 710055, China
email: sunbohua@xauat.edu.cn

The turbulent Poiseuille flow between two parallel plates is one of the simplest possible physical situations, and it has been studied intensively. In this paper, we propose a modified Prandtl-van Driest mixing length that satisfies both boundary conditions and wall damping effects. With our new formulations, we numerically solve the problem and, moreover, propose an approximate analytical solution of mean velocity. As applications of our solution, an approximate analytical friction coefficient of turbulent Poiseuille flow is proposed.

Keywords: Turbulent flow, Poiseuille flow, Prandtl mixing length, high heel velocity profile, Reynolds number

Contents

I. INTRODUCTION

The concept of the boundary layer was proposed by Prandtl in 1904 [1], initially he noticed that the fluid in the boundary layer is a laminar flow [2], firstly Prandtl and then von Kármán[3–5] realized that the flow inside the boundary layer can be either laminar and turbulent, or just turbulent. The boundary layer is a revolutionary concept in fluid mechanics, which has greatly promoted the development and application of fluid dynamics theory. Due to the uncertainty of the turbulent Reynolds stress, the proposed turbulent boundary layer equation still cannot be solved [1–36].

For the modeling of Reynolds stress, remarkable works include [16, 17], which shown that the Reynolds stress is a non local function in space of the time averaged velocity, involving an integral kernel, an extension of classical Boussinesq theory of turbulent viscosity. They do not use Prandtl mixing length but instead an equation for closure where the boundary condition is a consequence. Because of that they do not use a Prandtl equation, but instead an integral equation that reduces to a simpler one near the boundaries in a neighborhood defined precisely, a complete model where boundary conditions on the two walls are taken into account, however [16, 17] have not included the damping effects from both walls.

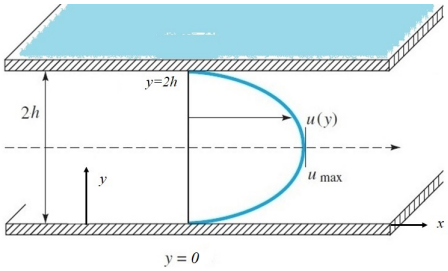

FIG. 1: Turbulent Poiseuille flow.

For the modeling of mean velocity profiles, notable works include [18, 20], which express wall constraint in terms of Lie-group dilation invariance of characteristic lengths, and yield a multi-layer structure of turbulent wall flows. Later, [19] extends the concept to all Reynolds stresses (including Reynolds shear stress and normal stresses), and yield a description for fluctuation velocity intensity profiles. Recently, regarding the Reynolds number scaling of near-wall fluctuations, [21] and [22] proposed the "law of bounded dissipation" and showed that near-wall peaks of turbulent dissipations, pressure intensities, fluctuation velocity intensities, etc. are all bounded for asymptotically high Reynolds numbers, differing from the view of infinite logarithmic growth by [23] and references therein.

The turbulent Poiseuille flow between two parallel plates as shown in Fig.1 is one of the simplest possible physical situations, and it has been studied intensively [7, 8]. Among those studies, in the first paper that

Preprints (www.preprints.org) | NOT PEER-REVIEWED | Posted: 14 December 2022 doi:10.20944/preprints202201.0240.v3

Prandtl proposed his mixing length model [5], for pipe flow, Prandtl assumed that the mixing length is proportional to $[(a-r)(a+r)]^{6/7}$, where a is pipe radius. His assumption implied that boundary conditions, $\ell(a)=0$, had been considered.

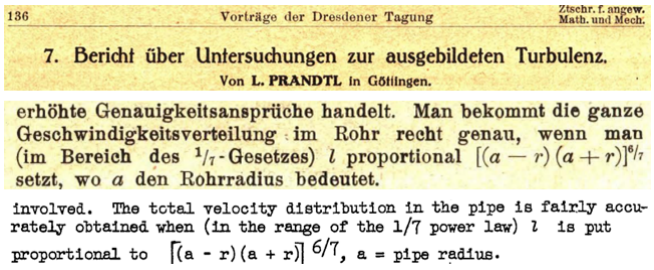

136 Vorträge der Dresdener Tagung Ztschr. f. angew. Math. und Mech.

7. Bericht über Untersuchungen zur ausgebildeten Turbulenz.

Von L. PRANDTL in Göttingen.

erhöhte Genauigkeitsansprüche handelt. Man bekommt die ganze Geschwindigkeitsverteilung im Rohr recht genau, wenn man (im Bereich des $^1/_7$-Gesetzes) l proportional $[(a-r)(a+r)]^{6/7}$ setzt, wo a den Rohrradius bedeutet.

involved. The total velocity distribution in the pipe is fairly accurately obtained when (in the range of the 1/7 power law) l is put proportional to $[(a-r)(a+r)]^{6/7}$, a = pipe radius.

FIG. 2: Quote and English translation from L. Prandtl, Bericht über Untersuchungen zur ausgebildeten Turbulenz, Z. Angew. Math. Mech. 5(2)(1925):136-139, which was the first paper of proposing the mixing length model.

In the masterpiece of H. Schlichting and K. Gersten [8], in Page 540, Eq. (17.71), for Couette flow (the Poiseuille flow is the special case of the Couette flow), they wrote, for lower wall, $\lim_{y\to 0}\ell=\kappa y$ and for upper wall, $\lim_{y\to 2h}\ell=\kappa(2h-y)$. Clearly, the boundary conditions at both lower and upper wall, $\ell(0)=0$ and $\ell(2h)=0$, have been used. Recently, Pomeau and Le Berre [17] studied the turbulent plane Poiseuille flow with mixing length $\ell=\kappa y(1-\frac{y}{2h})$, which is obtained from their expression $\ell=\kappa(h/2-z)(h/2+z)/h$ with transformation $z=y-h/2$ and $h/2\to h$, because their coordinate origin is in the middle and hight is h between two plates.

Van Driest [28] proposed a model that multiples the Prandtl mixing length ($\ell=\kappa y$) with a damping function $[1-\exp(-y/A)]$. However, van Driest model is only valid for the lower wall at $y=0$, but fails for the upper wall at $y=2h$. Absi [15] investigated the turbulent Poiseuille flow with a van Driest mixing length.

Therefore, it is still a great challenge to propose a mixing-length model that can give an accurate prediction in the whole domain of wall coordinates y. Furthermore, both analytical mean velocity profile and friction coefficient have not been formulated for the turbulent Poiseuille flow. We will study those problems in this paper.

The rest of this paper is organized as follows. In Section 2, we propose an enhanced Prandtl-van Driest mixing length. Section 3 completes formulations and we find integration solutions and an approximate analytical solution of mean motion. In Section 4, we obtain the approximate analytical friction of the turbulent Poiseuille flow between two parallel plates. Finally, conclusions are drawn in the last section.

II. ENHANCED PRANDTL–VAN DRIEST MIXING LENGTH

Here, we consider the turbulent Poiseuille flow (with density ρ and dynamical viscosity μ) between two parallel plates as shown in Fig.1, and we take the direction of the flow as the x axis and the plane of the surface as the xz plane, so y is the direction orthogonal to the surface. Assuming that the turbulent flow is steady with the pressure gradient along the x axis, the y and z components of the mean velocity are zero, and all of the quantities depend only on y. The pressure gradient drives against the shear stresses at the two walls.

According to the Prandtl mixing-length theory [5], the Reynolds stress is proposed to be

$$\tau'_{xy}=-\rho\overline{u'v'}=\rho\ell^2|\frac{d\bar{u}}{dy}|\frac{d\bar{u}}{dy}, \tag{1}$$

and or

$$\overline{u'v'}=\ell^2|\frac{d\bar{u}}{dy}|\frac{d\bar{u}}{dy}, \tag{2}$$

where u' and v' the velocity fluctuation components, ρ the flow density, $\bar{u}$ is the mean velocity.

The mixing length ℓ must have a length scale and simultaneously satisfies the boundary conditions, namely $\overline{u'v'}=0$ at both lower ($y=0$) and upper wall ($y=2h$); hence, we can propose the mixing length as follows:

$$\ell=\kappa y\varphi(y)\psi(y), \quad \text{and} \quad \varphi(2h)=0, \tag{3}$$

where κ is a numerical constant, namely, the von Kármán constant, in this paper we set $\kappa=0.4$; $\varphi(y)$ is a dimensionless function that may take a different format. To satisfy the boundary condition, the function φ can be proposed to be

$$y=2h:\ \varphi(2h)=(1-\frac{y}{2h})^{\gamma}=0, \tag{4}$$

where the parameter $\gamma>0$, Prandtl [5] set $\gamma=6/7$; for simplicity, we set $\gamma=1$ in the present work. Eq.4 is also used by Pomeau and Le Berre [17] to study the turbulent plane Poiseuille flow.

Regarding the determination of function $\psi(y)$, we must take into account the fixed-wall damping effects. We consider an infinite flat plate undergoing simple harmonic oscillation parallel to the plate in an infinite fluid. According to Stokes [37], the amplitude of the motion diminishes with increasing distance from the surface (wall) as a consequence of the lower-wall factor "$\exp(-\frac{y}{A})$" and upper wall factor "$\exp(-\frac{2h-y}{A})$", where A is a constant depending the frequency of oscillation of the plate and kinematic viscosity ν of the fluid [28].

Hence, in light of van Driest [28], we believe that when the plate is fixed and the fluid oscillates relative to the plate, the factor "$[1-\exp(-y/A)][1-\exp(-\frac{2h-y}{A})]$" must be applied to the fluid oscillation to obtain the damping

Preprints (www.preprints.org) | NOT PEER-REVIEWED | Posted: 14 December 2022 doi:10.20944/preprints202201.0240.v3

effect on both lower and upper wall. Furthermore, van Driest pointed out that fully developed turbulent motion occurs only beyond a distance sufficiently remote from the wall, and eddies are not damped by the nearness of the wall. Indeed, near a wall, the damping factor is

$$\psi = \psi_B \psi_T = [1 - \exp(-y/A)][1 - \exp(-\frac{2h - y}{A})], \quad (5)$$

for each mean velocity fluctuation, where the lower-wall van Driest damping function is

$$\psi_B = 1 - \exp(-\frac{y}{A}), \quad (6)$$

and the top-wall van Driest damping function is

$$\psi_T = 1 - \exp(-\frac{2h - y}{A}). \quad (7)$$

Therefore, to take into account the mean motion all the way to a smooth wall, the Prandtl mixing length could be proposed to the following form

$$\ell = \kappa y \varphi \psi = \kappa y \varphi \psi_B \psi_T. \quad (8)$$

Introducing dimensionless parameters

$$\begin{aligned} u_\tau &= \sqrt{\tau_w/\rho}, \\ y^+ &= y u_\tau/\nu, \\ u^+ &= \bar{u}/u_\tau, \\ Re_\tau &= h u_\tau/\nu, \end{aligned} \quad (9)$$

we have the dimensionless mixing length,

$$\ell^+ = \kappa y^+ \varphi^+ \psi^+, \quad (10)$$

where

$$\varphi^+ = 1 - \frac{y^+}{2Re_\tau}, \quad (11)$$

$$\psi^+(y^+) = [1 - \exp(-\frac{y^+}{A^+})][1 - \exp(-\frac{2Re_\tau - y^+}{A^+})], \quad (12)$$

and $A^+ = A u_\tau/\nu \approx 26$.

One might have a question, why do you need to consider the effects of both upper and lower walls? To answer this question, let's compare several different mixing length models for the case $Re_\tau = 1000$, as shown in Fig.3.

The interaction of the upper and lower boundaries can be clearly seen from the Fig.3. If you don't take the upper boundary into account as Prandtl model and van Driest model, the mixing length ℓ^+ is almost straight. If you consider the influence of the upper boundary, the mixing length ℓ is basically a parabola. Since flow is symmetrical to $y^+ = Re_\tau$, usually only half of it is studied such as $y^+ \in [0, Re_\tau]$, and even then the influence of the upper boundary needs to be taken into account, otherwise the mixing length ℓ^+ such as $\ell^+_{\text{Prandtl}} = \kappa y^+$ and $\ell^+_{\text{van Driest}} = \kappa y^+[1-\exp(-\frac{y^+}{A^+})]$, are not continue and have singularity at $y^+ = Re_\tau$, which is clearly not in line with the laws of physics. That is, even if only half of the flow is studied, a model that includes two boundary influences must be used. This is also consistent with a characteristic of the fluid, that is, the state of motion of one point is affected by points elsewhere.

With the above understanding, in the following sections, all solutions and discussions are based on the mixing length model in Eq.10 that is firstly proposed by this paper.

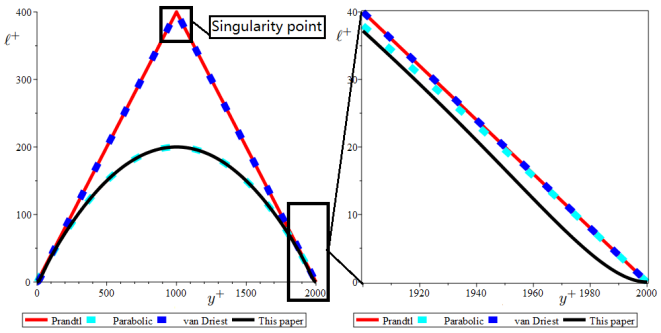

FIG. 3: The mixing-length profiles from different models at $Re_\tau = 1000$. Prandtl model $\ell^+_{\text{Prandtl}} = \kappa y^+$, Parabolic model $\ell^+_{\text{Prandtl Parabola}} = \kappa y^+(1 - \frac{y^+}{2Re_\tau})$, van Driest model $\ell^+_{\text{van Driest}} = \kappa y^+[1 - \exp(-\frac{y^+}{A^+})]$ and this paper's model $\ell^+_{\text{Sun}} = \kappa y^+(1 - \frac{y^+}{2Re_\tau})[1 - \exp(-\frac{y^+}{A^+})][1 - \exp(-\frac{2Re_\tau - y^+}{A^+})]$

III. FORMULATION AND SOLUTION OF MEAN MOTION

The Reynolds-averaged Navier-Stokes equations [10] of the turbulent Poiseuille flow under pressure gradient, $\frac{\partial p}{\partial x}$, are reduced to

$$\rho \frac{d\overline{v'^2}}{dy} + \frac{\partial p}{\partial y} = 0, \quad (13)$$

$$\mu \frac{d^2\bar{u}}{dy^2} - \rho \frac{d\overline{u'v'}}{dy} - \frac{\partial p}{\partial x} = 0, \quad (14)$$

and the boundary conditions, as shown in Fig.1, are

$$y = 0 : \bar{u} = 0, u' = 0, v' = 0, \text{ and } \mu \frac{d\bar{u}}{dy} = \tau_w \quad (15)$$

and

$$y = 2h : \bar{u} = 0, u' = 0, v' = 0, \text{ and } \mu \frac{d\bar{u}}{dy} = -\tau_w, \quad (16)$$

where $\bar{u}$ is the mean velocity, μ the dynamical viscosity, ρ the flow density, p the pressure, and u' and v' the velocity fluctuation components. The pressure gradient must be negative, namely, $\frac{\partial p}{\partial x} < 0$, to maintain the flow motion.

Preprints (www.preprints.org) | NOT PEER-REVIEWED | Posted: 14 December 2022 doi:10.20944/preprints202201.0240.v3

τ_w is the wall friction force on a unit area of the surface. This force is clearly in the x direction. The quantity τ_w is the constant flux of the x component of momentum transmitted by the fluid to the surface per unit time.

Integration of Eq.13 yields

$$\overline{v'^2} + \frac{p}{\rho} = \frac{p_0}{\rho}, \tag{17}$$

where p_0 is a function of x only [7]. Because $\overline{v'^2}$ is independent of x (by assumption), $\frac{\partial p}{\partial x}$ is equal to $\frac{dp_0}{dx}$. Both of these gradients should be independent of x to avoid streamwise acceleration of the flow [7]. Eq. 14 can be integrated to yield $\mu\frac{d\bar{u}}{dy} - \rho\overline{u'v'} = \frac{dp}{dx}y + C$. Applying the boundary condition in Eq.16, we have $\overline{u'v'} = 0$, leading to $C = \tau_w$. Hence, we have the following governing equation:

$$\nu\frac{d\bar{u}}{dy} - \overline{u'v'} = \frac{1}{\rho}\frac{dp_0}{dx}y + \frac{\tau_w}{\rho}, \tag{18}$$

where $\nu = \mu/\rho$ is kinematic viscosity.

Applying the boundary condition in 16, we have the relation between the wall friction and pressure gradient:

$$\frac{dp_0}{dx} = -\frac{\tau_w}{h}, \tag{19}$$

which indicates that the shear stress at the wall is determined by the pressure gradient and width of the channel only, which is one reason that this flow is less complicated than others [7]. Hence, Eq.18 is rewritten as

$$\nu\frac{d\bar{u}}{dy} - \overline{u'v'} = \frac{\tau_w}{\rho}(1 - \frac{y}{h}). \tag{20}$$

The first term on the left-hand side of Eq. 20 represents the effect of viscosity on the mean flow, whereas the second term is the Reynolds stress, namely, $\tau'_{xy} = -\rho\overline{u'v'}$. In turbulent flow located some distance away from a wall, the Reynolds stress is of considerably greater magnitude than the viscous stress; however, the role of viscous stress increases as the distance to a smooth wall decreases, until, finally, at the wall, viscosity predominates.

Applying the model in Eq.2, Eq. 20 becomes

$$\nu\frac{d\bar{u}}{dy} + \ell^2|\frac{d\bar{u}}{dy}|\frac{d\bar{u}}{dy} = \frac{\tau_w}{\rho}(1 - \frac{y}{h}), \tag{21}$$

which has two formats in different domains of y and each of them has its own solution.

(a) In the domain $y \in [0, h]$, we have $\frac{d\bar{u}}{dy}>0$, and the governing equation is

$$\nu\frac{d\bar{u}}{dy} + \ell^2(\frac{d\bar{u}}{dy})^2 = \frac{\tau_w}{\rho}(1 - \frac{y}{h}). \tag{22}$$

(b) In the domain $y \in [h, 2h]$, we have $\frac{d\bar{u}}{dy}<0$, and the governing equation is

$$\nu\frac{d\bar{u}}{dy} - \ell^2(\frac{d\bar{u}}{dy})^2 = \frac{\tau_w}{\rho}(1 - \frac{y}{h}). \tag{23}$$

With the dimensionless quantities in Eq.9, hence Eq.1 can be expressed as

$$\tau'^{+} = \frac{\tau'_{xy}}{\rho u_\tau^2} = (\ell^+)^2|\frac{du^+}{dy^+}|\frac{du^+}{dy^+}, \tag{24}$$

and Eq. 22 can be rewritten as

$$\frac{du^+}{dy^+} + (\ell^+)^2\left(\frac{du^+}{dy^+}\right)^2 = 1 - \frac{y^+}{Re_\tau}, \quad y^+ \in [0, Re_\tau], \tag{25}$$

and the boundary condition

$$y^+ = 0 : u^+ = 0. \tag{26}$$

The exact solution of Eq.25 that valid in the whole domain of y^+ has never been obtained, while only approximate asymptotic solutions have been proposed [7, 8], which caused a buffer problem between segmental solutions. Although the exact solution can not be found, its numeric integration can be carried out. For instance, [18] applied their own mixing length, derived a similar equation and found a numerical solution that valid in the whole domain by numeric integration.

From Eq.25, we can obtain

$$\frac{du^+}{dy^+} = \frac{2(1 - \frac{y^+}{Re_\tau})}{1 + \sqrt{1 + 4(\ell^+)^2(1 - \frac{y^+}{Re_\tau})}}. \tag{27}$$

Hence, the singularity-free solution is

$$u^+ = \int \frac{2(1 - \frac{y^+}{Re_\tau})}{1 + \sqrt{1 + 4(\ell^+)^2(1 - \frac{y^+}{Re_\tau})}}dy^+. \tag{28}$$

Similarly, Eq. 23 can be rewritten as

$$\frac{du^+}{dy^+} - (\ell^+)^2\left(\frac{du^+}{dy^+}\right)^2 = 1 - \frac{y^+}{Re_\tau}, \quad y^+ \in [Re_\tau, 2Re_\tau], \tag{29}$$

and its associated boundary condition

$$y^+ = 2Re_\tau : u^+ = 0. \tag{30}$$

From Eq.29, we can obtain

$$\frac{du^+}{dy^+} = \frac{2(1 - \frac{y^+}{Re_\tau})}{1 + \sqrt{1 - 4(\ell^+)^2(1 - \frac{y^+}{Re_\tau})}}. \tag{31}$$

Hence, the singularity-free solution is

$$u^+ = \int \frac{2(1 - \frac{y^+}{Re_\tau})}{1 + \sqrt{1 - 4(\ell^+)^2(1 - \frac{y^+}{Re_\tau})}}dy^+. \tag{32}$$

Preprints (www.preprints.org) | NOT PEER-REVIEWED | Posted: 14 December 2022 doi:10.20944/preprints202201.0240.v3

We can combine the derivatives in Eqs. (27) and (31) into a single form as follows:

$$\frac{du^+}{dy^+} = \frac{2(1-\frac{y^+}{Re_\tau})}{1+\sqrt{1-4(\ell^+)^2 \mid (1-\frac{y^+}{Re_\tau}) \mid}}, \quad y^+ \in [0, 2Re_\tau], \tag{33}$$

which is depicted in Fig. 4, showing that the velocity gradient is enormous near the wall, but decays rapidly to almost zero away from the wall. This is why the velocity profile near the wall must be obtained if we wish have a better understanding of the turbulent boundary layer.

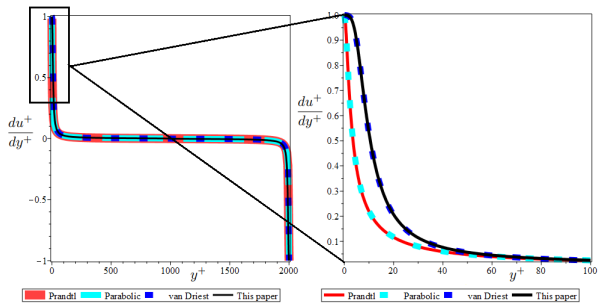

FIG. 4: Flow velocity gradient profile of turbulent Poiseuille flow at $Re_\tau = 1000$.

We can also combine the integral solutions in Eqs.(28) and (32) into a single form as follows:

$$u^+ = \int \frac{2(1-\frac{y^+}{Re_\tau})}{1+\sqrt{1+4(\ell^+)^2 \mid (1-\frac{y^+}{Re_\tau}) \mid}} dy^+. \tag{34}$$

To the best of our knowledge, the above integrations in the integral (34) cannot be completed exactly. Series solution can be integrated by parts, yielding

$$u^+ = \sum_{n=1}^{\infty} \frac{(-1)^n}{n!} (y^+)^n \frac{d^n u^+}{d(y^+)^n}, \tag{35}$$

where $\frac{du^+}{dy^+} = \frac{2(1-\frac{y^+}{Re_\tau})}{1+\sqrt{1-4(\ell^+)^2 \mid (1-\frac{y^+}{Re_\tau}) \mid}}$, and $\frac{d^2u^+}{d(y^+)^2} = \frac{d}{dy^+}(\frac{du^+}{dy^+}),..,\frac{d^n u^+}{d(y^+)^n} = \frac{d}{dy^+}(\frac{d^{n-1}u^+}{d(y^+)^{n-1}})$. This series solution can be computed to any order, but the series' convergence is poor and will need many terms to have a log law trend. We will not use this series solution in our computation.

Numerically, the integral in Eq.34 can be easily worked out for any Re_τ, and a Maple code was written to compute the integral; the results of Eq.34 are depicted in Fig. 5.

This shows that the flow velocity rapidly increases away from the wall and decreases close to the center of the channel and has a nice high heel profile.

It is worth noting that the log-rescale mean velocity has a nice high heel profile because the boundary conditions of both walls have benn taken into account. One would

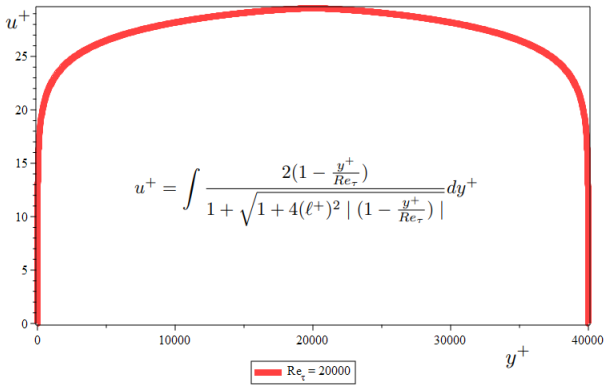

(a) Normal scale velocity profile

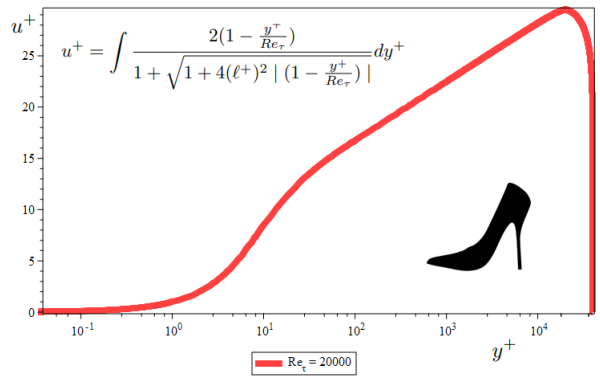

(b) Log-rescale velocity high heel profile

FIG. 5: The flow velocity profile of turbulent Poiseuille flow at $Re_\tau = 20000$. **a** Normal scale velocity profile; **b** Log-rescale velocity high heel profile,

not able to see the high heel profile if only one wall was considered. This high heel profile has never been seen in the literature before, and might be a universal feature of bounded flows.

Although the integral in Eq.34 cannot be completed exactly, we can try to obtain its approximate analytical solution. The author [32] obtained an exact closed form solution for plane turbulent flow: $\frac{du^+}{dy^+} + \kappa^2 (y^+)^2 \left(\frac{du^+}{dy^+}\right)^2 = 1$, under boundary condition: $y^+ = 0 : u^+ = 0$, its exact solution is given by: $u^+ = \frac{1}{\kappa} \ln(2\kappa y^+ + \sqrt{1+4\kappa^2 (y^+)^2}) - \frac{2y^+}{1+\sqrt{1+4\kappa^2 (y^+)^2}}$.

In light of the exact solution's structure obtained by author [32], we can propose an approximation of the integral (34) as follows:

$$u^+ \approx \frac{1}{\kappa} \ln\left[2\ell_*^+ + \sqrt{1+4(\ell_*^+)^2}\right] + \frac{\beta \ell_*^+}{1+\sqrt{1+4(\ell_*^+)^2}}, \tag{36}$$

Preprints (www.preprints.org) | NOT PEER-REVIEWED | Posted: 14 December 2022 doi:10.20944/preprints202201.0240.v3

where $\beta \approx 8.8$ and

$$\ell_*^+ = \kappa y^+ \varphi^+ \psi_*^+, \ \varphi^+ = 1 - \frac{y^+}{2Re_\tau}, \ A^+ = 26,$$
$$\psi_*^+ = [1 - \frac{4}{5}\exp(-\frac{y^+}{A^+})][1 - \frac{4}{5}\exp(-\frac{2Re_\tau - y^+}{A^+})]. \quad (37)$$

This approximate analytical solution in Eq.36 is valid in the whole domain $y^+ \in [0, 2Re_\tau]$, and has not been seen in the literature.

The solutions of Eqs. 34 and 36 are depicted in Fig. 6 and its log rescale is the high heel velocity profile.

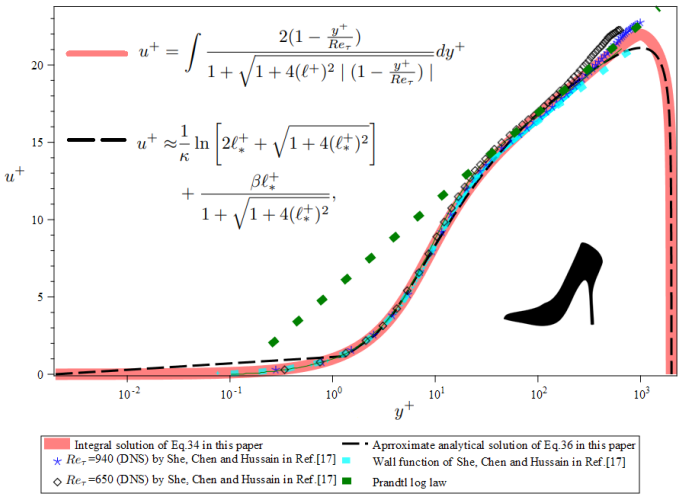

FIG. 6: The "high heel" velocity profile of turbulent Poiseuille flow at $Re_\tau = 1000$. Numerical integration solution in Eq. 34, approximate analytical solution in Eq. 36, DNS solutions [18], modelling [18] and Prandtl log law $u^+ = 2.5\log(y^+) + 5.5$.

Except for very small y^+, it is plausible to see that both the numerical integral solution in Eq.34 and approximate analytical solution in Eq.36 perfectly agree with direct numerical simulation (DNS) solutions [18] as well as modeling [18] in the domain of $y^+ \in [1, 2Re_\tau]$. Since [18] is the latest important result, the above validation shown that our results can be said to pass the test of [18].

For further validation, we compare the latest DNS results at $Re_\tau = 10000$ from [36] (as shown in Fig.7), which shows that our predictions from both numeric integral in Eq.34 and approximate analytical solution in Eq.36 are very well agree with the DNS results from [36].

It is worth pointing out that the latest and highest simulation result of this problem is up to $Re_\tau = 10000$, which is achieved by [36]. It is easily achieved by our formulations in Eq.34 and Eq.36, because our Re_τ is arbitrary number, for example, the result of $Re_\tau = 20000$ are shown in both Fig.5 and 7.

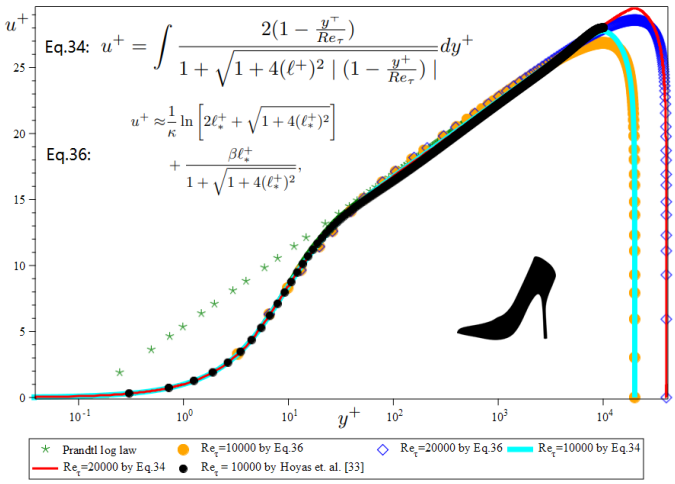

FIG. 7: The "high heel" velocity profile of turbulent Poiseuille flow at $Re_\tau = 10000$ and $Re = 20000$. Numerical integration solution in Eq. 34, approximate analytical solution in Eq. 36, DNS solutions [36] and Prandtl log law $u^+ = 2.5\log(y^+)+5.5$.

IV. FRICTION LAW OF TURBULENT POISEUILLE FLOW BETWEEN TWO PARALLEL PLATES

As an application of the proposed solutions, we now construct the dependence of the resistance/friction coefficient $c_f = \frac{\lambda}{4} = \frac{-2\tau_w}{\rho u_m^2} = \frac{2}{u_m^{+2}}$ or friction factor λ, leads to $u_m^+ = \sqrt{\frac{8}{\lambda}}$, where the velocity averaged over the cross-section is $u_m^+ = \frac{u_m}{u_\tau} = \frac{1}{2Re_\tau}\int_0^{2Re_\tau} u^+ dy^+$. Defining the Reynolds number $Re = \frac{2hu_m}{\nu} = 2Re_\tau\sqrt{\frac{2}{c_f}} = 2Re_\tau\sqrt{\frac{8}{\lambda}}$, which leads to $Re_\tau = \frac{1}{2}Re\sqrt{\frac{\lambda}{8}}$. With the above definitions, we have the friction law

$$\sqrt{\frac{8}{\lambda}} = \frac{1}{2Re_\tau}\int_0^{2Re_\tau} u^+ dy^+, \quad (38)$$

which produces an implicit form relation by an approximation of the mixing length $\ell^+ \approx \kappa y^+$ as conducting the above integration.

$$\sqrt{\frac{8}{\lambda}} \approx \frac{1}{\kappa}\ln(\kappa Re\sqrt{2\lambda}) + \frac{\beta}{2} - \frac{1}{\kappa} - \frac{\beta}{\kappa Re\sqrt{2\lambda}}\ln(1 + \kappa Re\sqrt{\frac{\lambda}{2}}), \quad (39)$$

For a large Reynolds number Re, the last term in Eq.39 can be omitted, hence the Eq.39 becomes

$$\sqrt{\frac{8}{\lambda}} \approx \frac{1}{\kappa}\ln(\kappa Re\sqrt{2\lambda}) - \frac{1}{\kappa} + 4.1, \quad (40)$$

which can be simplified into $\frac{1}{\sqrt{\lambda}} \approx 0.883883476\ln(Re\sqrt{\lambda}) + 0.062121857$ if set $\kappa = 0.4$ and $\beta = 8.8$.

Preprints (www.preprints.org) | NOT PEER-REVIEWED | Posted: 14 December 2022 doi:10.20944/preprints202201.0240.v3

Equation 39 and the Prandtl log-law, $1/\sqrt{\lambda} = 2\log(Re\sqrt{\lambda}) - 0.8$, as well as Zagarola and Smits [34], are depicted in Fig. 8.

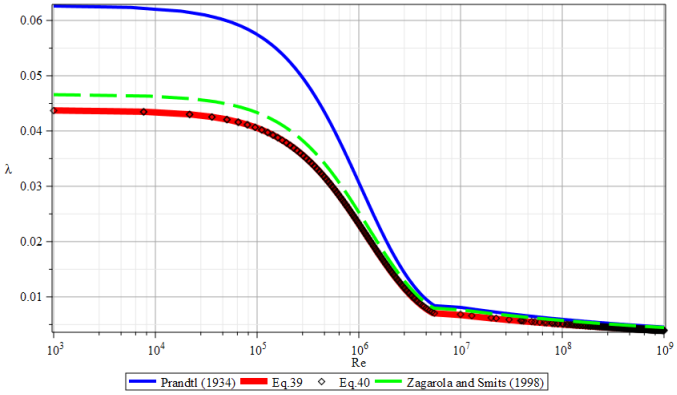

FIG. 8: Friction factor of turbulent Poiseuille flow between two parallel plates. It shows that the wall damping effects should be included.

The figure above shows that our coefficient of friction λ is below than Prandtl [8] and Zagarola and Smits [34]. The predictions here are in line with physics because our model includes both upper boundary conditions and damping effects, while the Prandtl [8] and Zagarola and Smits [34] only consider lower wall boundary conditions.

V. CONCLUSIONS

The study discovered that the mean velocity has the high heel profile, which might be a universal profile for all wall-bounded turbulent flows. The investigation confirmed that the correct mixing length formulae must include all boundary conditions together with damping functions by multiplication. This study may help facilitate a better understanding of turbulence phenomena [29–33].

Acknowledgments

This work was supported by Xi'an University of Architecture and Technology (Grant No. 002/2040221134). The author wishes to express his appreciation to Prof. Y. Pomeau for private communication and introduction of his work [17], Prof. X. Chen and Prof. Yun Bao for providing some useful publications, and to Mr. Zhe Liu for extracting the DNS, modelling and experimental data from Ref.[18], which are used to draw Fig. 6. Special thanks goes to my student, Mr. Xuang-Ting Liu, who modified the Maple code provided in the Appendix. I also wish to express my deep gratitude to all anonymous reviewers for their high-level academic comments that helped me to enhance the quality of this paper.

Statement on author contributions

Bo-Hua Sun created conceptualization, done all formulations, wrote Maple code, carried out numerical simulations and drawing, wrote the first draft of the manuscript and revised and edited the final version

Interest Conflict

The author declare that they have no conflict of interest.

Availability of data

The data supporting the findings of this study are available from the corresponding author upon reasonable request.

Maple Code of numeric integration of the integral in Eq. 34

Notes: In the Maple code, $c = Re_\tau$ and $\eta = y^+$. This code can be cut and pasted to Maple directly and run using Maple. The code produces normal scale of velocity profile, which can be easily converted into log rescale profile.

```
restart; with(student); with(plots); with(Student[Calculus1]); s := 1; kappa := 0.4; A := 26; a := 0; b := 0.02; c := 1000*s; R := 2*c; l := kappa*eta*(1 - eta/R)*(1 - exp(-eta/A))*(1 - exp(-(R - eta)/A)); for i to c do if a < 1 then a := a + b; elif 1 <= a and a < 10 then a := a + 10*b; elif 10 <= a and a < 100 then a := a + 100*b; elif 100 <= a and a < c then a := a + 1000*b; elif c <= a then break; end if; n[i] := int(2*(1 - 2*eta/R)/(1 + sqrt(1 + (4*l)*l*(1 - 2*eta/R))), eta = 0 .. a, numeric); end do; n[i - 1]; y1 := 0; for k to i - 1 do y1 := Matrix([y1, n[k]]); end do; y1 := Vector([y1]); y2 := n[i - 1]; for l from i - 2 by -1 to 1 do y2 := Matrix([y2, n[l]]); end do; y2 := Matrix([y2, 0]); y2 := Vector([y2]); a := 0; for j to c do if a < 1 then a := a + b; elif 1 <= a and a < 10 then a := a + 10*b; elif 10 <= a and a < 100 then a := a + 100*b; elif 100 <= a and a < c then a := a + 1000*b; elif c <= a then break; end if; m[j] := a; end do; x1 := 0; for k to i - 1 do x1 := Matrix([x1, m[k]]); end do; x1; x1 := Vector([x1]); meanvelocity[0*toR] := plot(x1, y1, legend = "This paper", thickness = 3, labels = [eta, "u+"], color = red, axes = boxed); a := c; for j to c do if c <= a and a < 2*c - 100 then a := a + 1000*b; elif 2*c - 100 <= a and a < 2*c - 10 then a := a + 100*b; elif 2*c - 10 <= a and a < 2*c - 1 then a := a + 10*b; elif 2*c - 1 <= a and a < 2*c then a := a + b; elif 2*c <= a then break; end if; m[j] := a; end do; x2 := c; for k to i - 1 do x2 := Matrix([x2, m[k]]); end do; x2; x2 :=
```

Vector([x2]); meanvelocity[Rto2R] := plot(x2, y2, legend = "This paper", thickness = 3, labels = [eta, "u+"], color = red, axes = boxed); y := Vector([y1, y2]); x := Vector([x1, x2]); meanvelocityinnormalscale := plot(x, y, legend = ["This paper"], thickness = 3, labels = [eta, "u+"], color = red, axes = boxed);

---

[1] Prandtl, L.: On fluid motions with very small friction. Third International Mathematical Congress, Heidelberg (1904).

[2] Blasius, H.: Grenzschichten in Fljssigkeiten mit kleiner Reibung. Z. Math. Phys. **56**, 1-37(1908).

[3] Prandtl, L.: Bemerkungen über die entstehung der turbulenz. Z. Angew. Math. Mech. **1**, 431-436(1921).

[4] von Kármán, Th.: Über leminere und turbulence Reibung (On Laminer and Turbulent Friction). Z. Angew. Math. Mech. **1**, 23(1921).

[5] Prandtl, L.: Bericht über Untersuchungen zur ausgebildeten Turbulenz. Z. Angew. Math. Mech. **5**,2, 136-139(1925).

[6] Prandtl, L. The mechanics of viscous fluids. In Aerodynamic Theory Vol III (ed. W. F. Durand), p. 130, 143. Julius Springer (1934).

[7] Tennekes, H. and Lumley, J.L.: A First Course of Turbulence. The MIT Press, Cambridge (1972).

[8] Schlichting, H. and Gersten, K.: Boundary Layer Theory (8th ed.) Springer, Berlin (2003).

[9] Landau, L.D. and Lifshitz, E.M.: Fluid Mechanics (2nd ed.) Butterworth-Heinemann (1987).

[10] Reynolds, O.: On the dynamical theory of incompressible viscous fluids and the determination of the criterion. Phil. Trans. Royal Soc. London. **186**, 123-164(1895).

[11] Millikan, C.M.: A critical discussion of turbulent flows in channels and circular tubes. Proc. of the Fifth Int. Cong. Appl. Mech., Wiley, New York (1939).

[12] Nikuradse, J.: Untersuchungen über turbulente Strömungen in nicht kreisförmigen Rohren. Ing. Arch. **1**, 306-332(1930).

[13] Nikuradse, J.: Gesetzmässigkeiten der turbulenten Stromung in glatten Rohren. Forschung auf dem Gebiet des Ingenieurwesens A. 44(1934).

[14] Baidya, R. Philip, J. Hutchins, N., Monty, J.P. and Marusic, I.: Distance-from-the-wall scaling of turbulent motions in wall-bounded flows. Phy.Fluids. **29**, 020712(2017).

[15] Absi, R.: A simple eddy visosity formulation for turbulent boundat payers near smooth walls. C.R. Mecanique, **337**, 158-165(2009).

[16] Pomeau Y. and Le Berre, M.: Turbulence in a wedge: the case of the mixing layer, Phys. Rev. Fluids. **6**, 074603 (2021).

[17] Pomeau, Y. and Le Berre, M.: Turbulent plane Poiseille flow, EPJ Plus. **136**, 1114(2021).

[18] She, Z.S. Chen, X. and Hussain, F.: Quantifying wall turbulence via a symmetry approach: A Lie group theory. J. Fluid, Mech. **827**, 322-356 (2017).

[19] Chen, X, Hussain, F. and She, Z.S.: Quantifying wall turbulence via a symmetry approach: Part II. Reynolds stresses. J. Fluid Mech. **850**, 401-438 (2018).

[20] Cantwell, B.J.: A universal velocity profile for smooth wall pipe flow. J. Fluid Mech. **878**, 834-874(2019).

[21] Chen, X. and Sreenivasan, K. R.: Reynolds number scaling of the peak turbulence intensity in wall flows. J. Fluid Mech. **908**, R3(2021)

[22] Chen, X. and Sreenivasan, K. R.: Law of bounded dissipation and its consequences in turbulent wall flows. J. Fluid Mech. **933**, A3(2022)

[23] Marusic, I. Baars, W.J. and Hutchins, N.: Scaling of the streamwise turbulence intensity in the context of inner-outer interactions in wall turbulence. Phys. Rev. Fluids. **2**, 100502(2017).

[24] Luchini, P.: Universality of the turbulent velocity profile. Phys.Rev.Lett. **118**, 224501(2017).

[25] Schlatter, P. Örlü, R. Li, Q., Brethouwer, G., Fransson, J.H.M., Johnsson, A.V., Alfredsson, P.H. and Henningson, D.S.: Turbulent boundary layers up to $Re_\theta = 2500$ studied through simulation and experiment. Phys. Fluids. **21**, 051702(2019).

[26] Spalart, P.R.: Direct simulation of a turbulent boundary layer up to $R_\theta = 1410$. J. Fluid Mech. **187**, 61-98(1988).

[27] Willert, C., Soria, J., Stanilas, M., Klinner, J., Amili, O., Eisfelder, M., Cuvier, C., Bellani, G., Fiorini, T. and Talamelli, A.: Near-wall statistics of a turbulent pipe flow at shear Reynolds numbers up to 40 000. J. Fluid Mech. , R5 (2017).

[28] van Driest, E.R.: On turbulent flow near a wall. J. Aeronaut. Sci. **23**(11), 1007-1011(1956).

[29] Sun, B.H.: The temporal scaling laws of compressible turbulence, Modern Physics Letters B. **30**(23), 1650297(2016).

[30] Sun, B.H.: Scaling laws of compressible turbulence, Appl. Math. Mech.-Engl. Ed. **38**(6), 765-778(2017) .

[31] Sun, B.H.: Thirty years of turbulence study in China. Appl. Math. Mech. -Engl. Ed. 40(2), 193-214(2019).

[32] Sun, B.H.: Revisiting the Reynolds-averaged Navier-Stokes equations, Open Physics. **19**, 853-862(2021).

[33] Sun, B.H.: Closed Form Solution of Plane-Parallel Turbulent Flow Along an Unbounded Plane Surface. Preprints, (2021) 2021110008 (doi: 10.20944/preprints202111.0008.v4).

[34] Zagarola, M.V. and Smits, A. J. Mean-flow scaling of turbulent pipe flow. J. Fluid Mech. **373**:33-79 (1998).

[35] Lee, M. and Moser, R. D. Direct numerical simulation of turbulent channel flow up to $Re_\tau \approx 5200$. Journal of Fluid Mechanics, **774**:395-415(2015).

[36] Hoyas, S., Oberlack, M., Alcántara-Ávila, F.: Wall turbulence at high friction Reynolds numbers. Phy.Rev.Fluids **7**, 014602 (2022).

[37] Stokes, G.G.: On the effect of the internal friction of fluids on the motion of pendulums, Trans. Cambridge Philos. Soc. **9** (1851).